ACS APPLIED MATERIALS & INTERFACES

Research Article

www.acsami.org

Hemocompatibility of Poly(vinyl alcohol)–Gelatin Core–Shell Electrospun Nanofibers: A Scaffold for Modulating Platelet Deposition and Activation

Valerie M. Merkle,[†] Daniel Martin,[‡] Marcus Hutchinson,[§] Phat L. Tran,[∥] Alana Behrens,[‡] Samir Hossainy,[∥] Jawaad Sheriff,[⊥] Danny Bluestein,[⊥,#] Xiaoyi Wu,*[,†,#] and Marvin J. Slepian*[,†,‡,∥,⊥]

[†]Biomedical Engineering Graduate Interdisciplinary Program, The University of Arizona, Tucson, Arizona 85721, United States

[‡]Department of Biomedical Engineering, The University of Arizona, Tucson, Arizona 85721, United States

[§]Department of Molecular and Cellular Biology, The University of Arizona, Tucson, Arizona 85721, United States

[∥]Sarver Heart Center, Department of Medicine, The University of Arizona, Tucson, Arizona 85721, United States

[⊥]Department of Biomedical Engineering, Stony Brook University, Stony Brook, New York 11794, United States

[#]Aerospace & Mechanical Engineering Department, The University of Arizona, Tucson, Arizona 85721, United States

ABSTRACT: In this study, we evaluate coaxial electrospun nanofibers with gelatin in the shell and poly(vinyl alcohol) (PVA) in the core as a potential vascular material by determining fiber surface roughness, as well as human platelet deposition and activation under varying conditions. PVA scaffolds had the highest surface roughness (Ra = 65.5 ± 6.8 nm) but the lowest platelet deposition (34.2 ± 5.8 platelets) in comparison to gelatin nanofibers (Ra = 36.8 ± 3.0 nm and 168.9 ± 29.8 platelets) and coaxial nanofibers (1 Gel:1 PVA coaxial, Ra = 24.0 ± 1.5 nm and 150.2 ± 17.4 platelets. 3 Gel:1 PVA coaxial, Ra = 37.1 ± 2.8 nm and 167.8 ± 15.4 platelets). Therefore, the chemical structure of the gelatin nanofibers dominated surface roughness in platelet deposition. Due to their increased stiffness, the coaxial nanofibers had the highest platelet activation rate, rate of thrombin formation, in comparison to gelatin and PVA fibers. Our studies indicate that mechanical stiffness is a dominating factor for platelet deposition and activation, followed by biochemical signals, and lastly surface roughness. Overall, these coaxial nanofibers are an appealing material for vascular applications by supporting cellular growth while minimizing platelet deposition and activation.

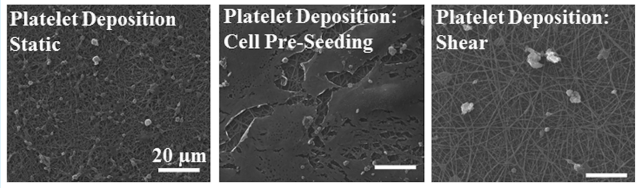

KEYWORDS: *Platelets, Gelatin, Poly(vinyl alcohol), Coaxial Electrospinning, Tissue Engineering*

1. INTRODUCTION

Cardiovascular disease is the leading cause of mortality in the United States.[1] The underlying pathology for cardiovascular disease remains obstructive atherosclerotic coronary artery disease (CAD).[2] To overcome coronary obstruction, revascularization, either via percutaneous balloon angioplasty stenting or surgical bypass graft surgery, is utilized.[3−5] In the United States, over 600 000 angioplasty and stent procedures[6] and 1.4 million coronary artery bypass procedures[2] are performed yearly. Despite the success of both of these approaches, they remain limited by progressive arterial or bypass graft reclosure. Vessel reclosure for both of these approaches involves localized thrombosis or neointimal thickening with smooth muscle cell migration and proliferation.[3−5] As a result, a need exists for materials and strategies that may be applied to arterial stents or bypass graft veins that may modulate localized thrombosis. Further, development of novel hemocompatible materials may extend our therapeutic capability to accelerate localized endothelialization thereby limiting thrombosis and neointimal thickening.[3−5,7]

To further improve the materials and devices that come into direct contact with blood, various modifications such as coatings and drug incorporation have been made. For example, several stent coatings such as gold,[8−11] silicon carbide,[9−12] and phosphorylcholine[9−12] have been investigated; however, these coatings do not show any discernible improvement in restenosis for coronary applications. Additionally, drugs such as heparin[9,10] and corticosteroids[13,14] have been incorporated into the stents in an attempt to further decrease restenosis rates. The use of these drugs did not show a statistically significant difference when compared to the bare metal stent counterparts.[9,10,13,14] Furthermore, stents can be covered with a graft material such as expanded polytetrafluoroethylene (PTFE),[15−17] polyethylene terephthalate (PET),[15] or polyurethane (PU)[15,18,19] that provides a physical barrier between the stent and the vessel wall. Therapeutic agents can be incorporated into the graft to provide a more uniform release

Received: February 22, 2015
Accepted: March 27, 2015
Published: March 27, 2015

DOI: 10.1021/acsami.5b01671
ACS Appl. Mater. Interfaces 2015, 7, 8302−8312

distribution across the entire stent−graft area. Surface modifications in the graft material, itself, can also be made to tailor the stent−graft for a given indication. These surface modifications include biomimetic peptides, antibodies, growth factors, and nanoparticles.[15]

The use of a nanofibrous material is a novel method for formation of a physical barrier between the bloodstream and the tissue, offering a potential utility as coating materials for stents or structural materials for application to or fabrication of vascular grafts. Recent advances in tissue engineering have yielded several approaches for forming fibrous scaffolds. In particular, the process of electrospinning forms fibrous scaffolds with diameters ranging from the micrometer to nanometer scale.[20,21] These electrospun scaffolds have high specific surface areas, porosities, as well as features on the micro- to nanoscale.[22,23] Dual- or multiple-component fibers can also be fabricated that have a set of properties that the single component fibers may not have. For example, scaffolds that are used for vascular applications need both mechanical strength and high biocompatibility.[22,23] Scaffolds composed of materials with dominant biological properties have high biocompatibility but often have poor mechanical properties.[24−29] In contrast, synthetic polymer scaffolds have appealing mechanical properties; however, they lack biological properties due to their insufficient cellular recognition sites.[24−27]Therefore, creation of composite fibers can combine the mechanical properties of the synthetic polymers and the biological properties of the natural polymer. In addition, therapeutic agents, growth factors, and other proteins can be incorporated or chemically bound to the fibers in order to tailor the scaffold to a given application. Incorporation of the therapeutic agents into the fibers allows these agents to be released locally.[30−33]

In this study, we fabricate coaxial nanofibers with poly(vinyl alcohol) (PVA) in the core and gelatin in the shell of each fiber. PVA is a semicrystalline, hydrophilic, and synthetic polymer that has displayed mechanical properties similar to soft tissue.[34] In contrast, gelatin, a product of collagen hydrolysis, has high biocompatibility but poor mechanical properties.[28,35,36] Therefore, combining these materials in a core−shell structure allows the fibers to have the structural benefit of PVA in the core and the biological benefit of gelatin in the shell.[37]

For any material to be a successful construct in the vasculature, hemocompatibility is of vital importance. The first stage of the hemostatic response of platelets is surface deposition.[38] Therefore, we evaluate platelet deposition on the electrospun scaffolds under static conditions, mechanical activation (using a hemodynamic shearing device[39]), chemical activation (using adenosine diphosphate[40,41]), and shear conditions (using a parallel plate flow chamber[42]), respectively. Surface roughness is an important factor affecting hemocompatibility, meaning that a rougher surface with higher exposed surface area leads to more rapid blood coagulation.[43] Thus, atomic force microscopy (AFM) is utilized to determine fiber surface roughness, which may play a role in platelet deposition and subsequent platelet activation on the electrospun nanofibers. Additionally, we seek to elucidate the effect of biochemical signals on platelet deposition and activation. In this study, we compare PVA, a synthetic polymer, and gelatin, a biocompatible polymer, for platelet deposition and subsequent activation.

After platelet deposition, platelet activation is the next step in the hemostatic response.[38] To determine platelet activation on the electrospun nanofibers, we utilized a modified prothrombinase assay[44−46] that calculated the rate of thrombin formation. Thus, the rate of thrombin formation is directly related to the activation of platelets.[44−46] Platelets can sense the mechanical stiffness of the underlying substrate, leading to an increase in activation on stiffer surfaces.[47] Our previous work has shown the increase in mechanical stiffness of the coaxial (gelatin in the shell and PVA in the core) nanofibers in comparison to scaffolds composed solely of gelatin or PVA.[37,48] This work has also shown favorable biocompatibility with the coaxial scaffolds promoting 3T3 fibroblast viability and proliferation.[37,48] Thus, we seek to determine platelet deposition when scaffolds are preseeded with smooth muscle cells or human umbilical vein endothelial cells, cells native to the vasculature. Therefore, we hypothesize that the coaxial nanofibers with gelatin in the shell and PVA in the core of each fiber will be an optimal construct for vascular applications due to its support for cellular viability and proliferation by displaying minimal platelet deposition and activation.

2. EXPERIMENTAL SECTION

2.1. Electrospinning. A 16% w/v solution of PVA (Sigma-Aldrich, 89 000−98 000 MW, 99+% hydrolyzed) was prepared with ethanol and water (1:9 v/v) in a water bath for 4 h at 60 °C. The use of ethanol and water as solvents increased the evaporability of solvents for subsequent electrospinning compared to using only water as a solvent. Electrospun PVA nanofibers were fabricated from a custom-built electrospinning device using the following parameters: 12 kV applied high voltage (Acopian High Voltage Power Supply), 12 cm fixed needle-tip to collector distance, and 9 μL/min fixed flow rate (Razel Syringe Pump, R-99). A 15% w/v solution of Gelatin Type A (Sigma-Aldrich) was prepared from ethanol and 10×-phosphate buffered saline (PBS) (1:1 v/v) in a water bath for 2 h at 40 °C and subsequently at room temperature for 12 h for further dissolution. Gelatin nanofibers were fabricated using the following parameters: 12 kV applied voltage, 12 cm fixed needle-tip-to-collector distance, and a 30 μL/min flow rate. The coaxial nanofibers were fabricated using a custom-coaxial electrospinning device using the previously described gelatin and PVA solutions. Composite fibers were made using two different flow rate conditions: 3 Gel:1 PVA (3 μL/min flow rate for PVA and 9 μL/min flow rate for gelatin) and 1 Gel:1 PVA (7 μL/min for gelatin and PVA, respectively). Each composite scaffold used a 20 kV applied voltage and 15 cm needle-tip-to-collector distance. After electrospinning was complete, all scaffolds were then cross-linked using a glutaraldehyde/ethanol vapor. To cross-link the scaffolds, a 5% glutaraldehyde in ethanol solution was prepared and placed in the bottom of a desiccator. Next, the scaffolds were placed on the desiccator shelf and vacuum was pulled. The desiccator was then placed in an oven at 42 °C for 20 h. After the 20 h in the oven, the scaffolds were ready for subsequent experiments as described in the proceeding sections.

2.2. Fiber Surface Roughness. The samples were gold coated under argon gas at 70 mTorr for 60 s. The samples were imaged in a Bruker dimensional atomic force microscopy (AFM) using tapping mode. The surface roughness (Ra) was determined using the Bruker Nanoscope Analysis v1.40r2 software for 25 fibers of each scaffold (gelatin, PVA, 1 Gel:1 PVA coaxial, and 3 Gel:1 PVA coaxial). The images were corrected using the 3rd order-flattening tool to remove tilts and bows from the images. The roughness (Ra) values were obtained using the roughness tool with the peak inputs on. The peak inputs allowed us to define a threshold height from the surface to measure the roughness. This ensured that only the roughness of the fiber was obtained.

2.3. Blood Samples. Blood samples were taken from healthy adults who signed informed consent forms. Adults did not take aspirin or ibuprofen for 2 weeks prior to donating and had not consumed caffeine for 12 h prior to blood draw. Thirty milliliters of whole blood was drawn via venipuncture and added to 0.3 mL 40% trisodium

DOI: 10.1021/acsami.5b01671
ACS Appl. Mater. Interfaces 2015, 7, 8302−8312

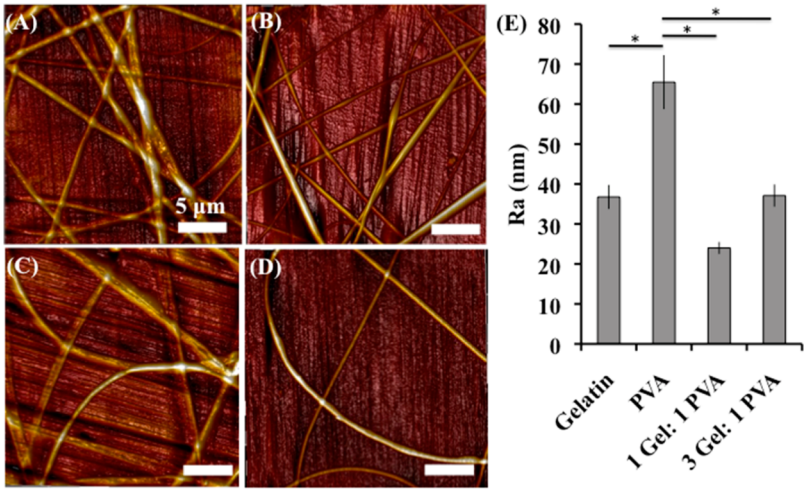

Figure 1. Fiber surface roughness was assessed using atomic force microscopy (AFM) for (A) gelatin scaffolds, (B) PVA scaffolds, (C) 1 Gel:1 PVA coaxial scaffolds, and (D) 3 Gel:1 PVA coaxial scaffolds. Surface roughness values are presented as Ra (nm) in the table (panel E). Asterisk (*) indicates significance with $p < 0.001$.

citrate. The whole blood was centrifuged at 450*g* for 4.5 min. The platelet-rich plasma (PRP) was removed from the sample. The PRP was filtered through a 150 mL column of Sepharose 2B beads (2% agarose; Amersham-Pharmacia, Sigma Chemical, St. Louis, MO) to yield the gel-filtered platelets (GFP).

2.4. Platelet Viability. Platelet viability was assessed using a lactate dehydrogenase (LDH) assay (Thermo Scientific) after 3 h of incubation on the electrospun scaffolds or tissue culture plate (TCP) according to manufacturer's instructions.

2.5. Platelet Deposition on Electrospun Scaffolds. Five hundred microliters of 20 000 platelets/μL was incubated on the scaffold or substrate surface. Platelets and scaffolds were incubated at 37 °C, 5% CO_2, and 95% relative humidity for 4 h. After incubation, platelets were fixed for scanning electron microscopy (SEM) using 5% glutaraldehyde. The cells/scaffolds were then transferred from glutaraldehyde (GTA) to deionized water through a series of graded solutions (3 GTA:1 H_2O, 1 GTA:1 H_2O, and 1 GTA:3 H_2O). Next, solutions were transferred to ethanol (EtOH) using a series of graded solutions (3 H_2O:1 EtOH, 1 H_2O:1 EtOH, and 1 H_2O:3 EtOH) and allowed to sit overnight in the ethanol solution. Lastly, the samples were transferred to hexamethyldisilazane (HMDS) through a series of graded solutions (3 EtOH:1 HMDS, 1 EtOH:1 HMDS, and 1 EtOH:3 HMDS) and then allowed to air-dry overnight.[49] After preparation, the samples were gold-coated for 60 s using a sputter coater and imaged using field emission scanning electron microscopy (SEM, Hitachi-S4800). Platelet deposition on scaffolds was determined using the National Institute of Health's ImageJ software using ten images for each scaffold type.

For the mechanically activated platelets, platelets at a concentration of 20 000 platelets/μL were subjected to a physiological shear of 10 dyne/cm^2 for 10 min using the hemodynamic shearing device.[39] Platelets were then seeded onto the scaffolds and incubated for 4 h as described in the preceding paragraph. After the 4 h of incubation, the scaffolds were prepared for SEM imaging as previously described.

For the chemically activated platelets, platelets at a concentration of 20 000 platelets/μL and 5 μM adenosine diphosphate (ADP) were incubated on each scaffold for 4 h. Samples were prepared for SEM imaging as described previously.

2.6. Platelet Activation Assay. Platelet activation state (PAS) was measured using a chemically modified prothrombinase-based assay. Each scaffold was seeded with 500 μL of human platelets at a concentration of 20 000 platelets/μL in platelet buffer. Samples were incubated at 37 °C for 0, 60, 120, and 180 min. After incubation, 200 nM Factor IIa (acetylated prothrombin), 100 pM factor Xa, and 5 mM calcium (Ca^{2+}) were added and incubated for 10 min. After the 10 min incubation, samples were read at 405 nm for 7 min in a plate reader at 405 nm to obtain the PAS values. The PAS values at each time point were normalized against fully activated platelets (obtained using 7.5 W of sonication for 10 s). The normalized value represents the fraction of thrombin that is produced by fully sonicated platelets. The platelet activation rate (PAR) is obtained from the slope of the PAS values over 3 h.[44−46]

2.7. Platelet Deposition under Flow Conditions. Platelet deposition on the electrospun scaffolds was determined under vascular relevant shear conditions to better simulate the in vivo environment. Platelet-rich plasma was diluted to a concentration of 15 000 platelets/μL and circulated for 60 min across the scaffold surfaces at 1 or 3 dyn/cm^2, respectively. The samples were then fixed and imaged using a SEM in order to determine platelet deposition.

2.8. Effects of SMC or HUVEC Preseeding on Platelet Deposition. To prepare the scaffolds for cell culture, the scaffolds were placed in an oven at 42 °C for a period of 24 h. Next, the scaffolds were sterilized in the ultraviolet light for 30 min prior to cell culture. The scaffolds were then incubated with cell culture media for a period of 15 min prior to cellular seeding. Cell culture media for human umbilical vein endothelial cells (HUVEC) was M-199 stock media supplemented with 1% 0.2 M glutamine, 1.5% 1 M HEPES (Lonza Walkersville, Walkersville, MD, USA), 7.5% $NaHCO_3$, 1.8% penicillin/streptomycin/gentamicin (Lonza Walkersville, Walkersville, MD, USA), 15% fetal calf serum (Lonza Walkersville, Walkersville, MD, USA), heparin salt (Fisher Bioreagants, Fair Lawn, NJ, USA) and ECGS (endothelial cell growth supplements). Human umbilical vein endothelial cell (HUVEC) (BD Biosciences, San Jose, CA, USA) were grown to 80% confluency and were passaged using a 1:1 mixture of trypsin−versene and HBSS (Lonza Walkersville, MD, USA).

Cell culture media for the primary smooth muscle cells (SMC) was Dulbecco's modified Eagle's medium (Life Technologies, Carlsbad, CA, USA) supplemented with 10% v/v fetal calf serum (Life Technologies, Carlsbad, CA, USA), antibiotic/antimycotic (Life Technologies, Carlsbad, CA, USA), and 1% 0.2 M L-glutamine (Lonza Walkersville, Walkersville, MD, USA). The primary smooth muscle cells were isolated from the aorta of an adult, male Sprague−Dawley rat. SMC were also grown to 80% or higher confluency and passaged using trypsin−versene.

After incubation with the cell culture media, the respective cell line was seeded on the scaffold and incubated at 37 °C, 5% CO_2, and 95% relative humidity for 3 days with the media refreshed on day 2. As a control, cells were seeded on the tissue culture polystyrene well (TCP) without any scaffolds present, as well as a gelatin film coated on the tissue culture polystyrene well.

After the 3 days of incubation, the scaffolds were rinsed three times with 1× phosphate-buffered saline (PBS) and once with platelet buffer.

DOI: 10.1021/acsami.5b01671
ACS Appl. Mater. Interfaces 2015, 7, 8302−8312

After rinsing with platelet buffer, the scaffolds were seeded with platelets at a concentration of 20 000 platelets/μL for 4 h. After incubation, platelet deposition on the cell-coated scaffolds was determined as previously described.

2.9. Statistical Analysis. All results are presented as mean ± standard error unless otherwise indicated. Statistical analysis was completed using a two-tailed, unpaired student's t test.

3. RESULTS AND DISCUSSION

3.1. Fiber Surface Roughness. For a material to be a successful vascular construct, the material must be evaluated to ensure low platelet activation while maintaining the platelet's role in hemostasis and angiogenesis.[50] Enhanced surface roughness increases platelet adhesion and the presence of platelet pseudopodia to the underlying substrate. Therefore, there is an increase in platelet adhesion, spreading, and subsequent platelet activation.[51,52] In this experiment, we first sought to determine the fiber surface roughness of the gelatin, PVA, and coaxial nanofibers (1 Gel:1 PVA coaxial and 3 Gel:1 PVA coaxial) because this parameter plays a role in platelet adhesion and subsequent activation.

A Bruker atomic force microscope and the Bruker Nanoscope Analysis software were utilized to determine the surface roughness of individual nanofibers (Figure 1). The fiber surface roughness is reported as Ra, representing the average surface height deviations from a given reference point (i.e., the surface of the stainless steel chip that the fibers are electrospun onto). The use of the reference point allows us to determine the surface roughness of each individual fiber without taking into account the stainless steel substrate that the fibers were electrospun on. Out of all of the fibers, PVA had the highest surface roughness (Ra = 65.5 ± 6.8 nm) when compared to gelatin ($p < 0.001$), 1 Gel:1 PVA coaxial scaffolds ($p < 0.001$), and 3 Gel:1 PVA coaxial scaffolds ($p < 0.001$). This led us to the question: does the increased surface roughness of the PVA nanofibers lead to an increase in platelet deposition and activation in comparison to the less rough fibers of gelatin and the coaxial nanofibers? We utilized these fiber surface roughness values into the proceeding analyses for platelet deposition and activation.

3.2. Platelet Viability on Electrospun Nanofibers. Platelet viability was determined using a lactate dehydrogenase (LDH) assay.[53,54] Damage to the cell membrane causes lactate dehydrogenase to leak into the platelet buffer. The LDH now in the media can then convert the pyruvate to lactate through the reduction of NAD^+ to NADH. With NADH now present, the diaphorase can then convert tetrazolium salt to red formazan, which can then be quantified using a spectrophotometer at a wavelength of 490 nm. All scaffolds (gelatin, PVA, 1 Gel:1 PVA coaxial, and 3 Gel:1 PVA coaxial) and the tissue culture polystyrene plate (TCP) possessed platelet viability of 98+% at hours 1, 2, and 3 of incubation (Figure 2). Therefore, the scaffold surfaces promote platelet viability throughout all subsequent platelet deposition and activation studies.

3.3. Platelet Deposition on Electrospun Nanofibers under Static Conditions. Platelet deposition after incubation was calculated using SEM images (3000× magnification, approximately 8400 μm^2) and the National Institute of Health's ImageJ software (Figure 3). The gelatin scaffolds (169 ± 30 platelets) and the coaxial scaffolds (1 Gel:1 PVA coaxial, 150 ± 17 platelets; 3 Gel:1 PVA coaxial scaffold, 168 ± 15 platelets) possessed similar platelet deposition and significantly more platelets than the PVA scaffolds (34 ± 6 platelets). Despite the PVA fibers' having the highest surface roughness, these fibers had the lowest platelet deposition out of all of the scaffolds. Gelatin, rich in cellular attachment sites, has higher platelet deposition than the PVA fibers with significantly higher surface roughness and lacking cellular attachment sites. Therefore, surface roughness was not a dominating factor in platelet deposition. The chemical signals present on the biocompatible gelatin fibers were a dominant factor in platelet deposition in comparison to the synthetic polymer PVA, lacking these cellular recognition sites.

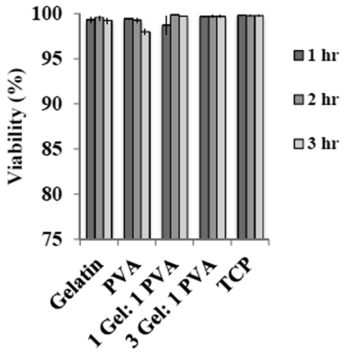

Figure 2. Platelet viability assessed using a lactate dehydrogenase (LDH) assay after 3 h of seeding on gelatin scaffolds, PVA scaffolds, 1 Gel:1 PVA coaxial scaffolds, 3 Gel:1 PVA coaxial scaffolds, and tissue culture plate (TCP).

3.4. Platelet Activation on Electrospun Scaffolds under Static Conditions. In addition to platelet deposition, platelet activation is an important determinant of a material's hemocompatibility and potential to serve as a vascular construct. Activated platelets in the presence of factor II (prothrombin) and factor Xa form a prothrombinase complex that catalyzes the conversion of prothrombin to thrombin. In the normal coagulation cascade, thrombin formation provides a positive feedback on the activation of platelets and additional thrombin formation.[44] Therefore, quantification of platelet activation using thrombin can be difficult. In this study, we utilize a modified prothrombinase assay in which acetylated prothrombin is utilized. Essentially, this assay determines the quantity of acetylated thrombin formed from acetylated prothrombin using low platelet concentrations (20 000 platelets/μL). Use of the acetylated prothrombin at low platelet concentrations inhibits the positive feedback of the thrombin formation on the platelets. Thus, a 1:1 correlation is achieved between platelet activation and acetylated thrombin formation.[44]

Electrospun scaffolds were incubated with 500 μL of platelets at a concentration of 20 000 platelets/μL for 0, 1, 2, or 3 h. If the platelets are activated from the interaction with the nanofibers, then the anionic phospholipid (phosphatidylserine) is translocated from the inner leaflet to the outer leaflet of the cell membrane. Phosphatidylserine will then bind and activate coagulation factors VII, IX, X, and prothrombin. Additionally, activated platelets will activate factor V, present in the α-granules, and express it on the membrane surface. Activated factor V is required for the factor Xa activation of prothrombin. Therefore, activated platelets produce the necessary cofactors needed for the formation of acetylated prothrombin, which is measured in subsequent steps of this assay.[44]

At each time point (t = 0, 60, 120, or 180 min), acetylated factor II, factor Xa, and Ca^{2+} were added to the well and incubated at 37 °C for 10 min to start the assay. After the 10

DOI: 10.1021/acsami.5b01671
ACS Appl. Mater. Interfaces 2015, 7, 8302−8312

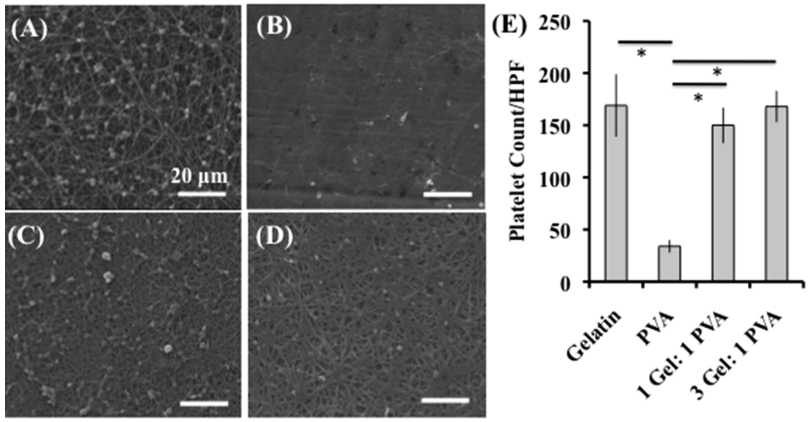

Figure 3. Platelet deposition under static conditions on electrospun scaffolds (A) gelatin, (B) PVA, (C) 1 Gel:1 PVA coaxial, and (D) 3 Gel:1 PVA coaxial. Platelet deposition per HPF (high-powered field 3000× magnification, approximately 8400 μm^2) for each of the electrospun scaffolds is depicted (E). Scale bar is 20 μm. Asterisk (*) indicates significance with $p < 0.001$.

min incubation, a chromogenic substrate (Chromozyme-TH) for thrombin is added, which allows the amount of acetylated thrombin to be quantified in a plate reader at 405 nm for 7 min. The slope of the absorbance over the 7 min reading is referred to as platelet activation state (PAS). The PAS values are normalized with the PAS value obtained for fully activated platelets. Therefore, the normalized PAS value represents the fraction of acetylated thrombin formed from fully activated platelets. The platelet activation rate (PAR) is the slope of the individual PAS values at each time point throughout the modified prothrombinase assay (0, 1, 2, and 3 h), which indicates the overall rate of change of platelet activation. Therefore, the PAR indicates how rapidly the platelets are becoming activated when in the presence of the electrospun scaffolds. Overall, the PAR is used for comparison of platelet activation between the scaffolds.

The PAS of the platelets on the scaffolds (gelatin, PVA, 1 Gel:1 PVA coaxial, and 3 Gel:1 PVA coaxial), as well as the tissue culture plate (TCP) are calculated and presented in Figure 4A. The platelet activation rate (PAR) is calculated from the PAS values for each scaffold and the TCP over the 3 h of incubation, and we utilized this value for comparison between substrates. When the platelets were incubated on the scaffold or TCP surfaces, the platelet activation rate was highest for the TCP when compared with the gelatin scaffolds ($p = 0.004$), PVA scaffolds ($p = 0.002$), 1 Gel:1 PVA coaxial scaffolds ($p = 0.06$), and 3 Gel:1 PVA coaxial scaffolds ($p = 0.03$) (Figure 4B). The coaxial scaffolds (1 Gel:1 PVA and 3 Gel:1 PVA) had similar PAR ($p = 0.52$). The 1 Gel:1 PVA coaxial scaffold had higher PAR when compared to gelatin ($p = 0.045$) and PVA ($p = 0.03$); however, results were less significant when comparing the 3 Gel:1 PVA coaxial scaffolds with gelatin ($p = 0.12$) or PVA ($p = 0.08$).

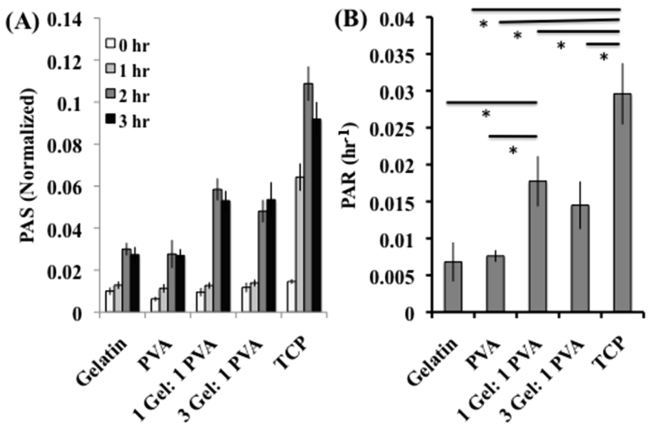

Figure 4. (A) Platelet activation state (PAS) and (B) platelet activation rate (PAR) of platelets incubated under static conditions on the scaffolds (gelatin, PVA, 1 Gel:1 PVA coaxial, and 3 Gel:1 PVA coaxial) and the tissue culture plate (TCP). Platelet activation correlates with mechanical stiffness of underlying substrate: stiffer substrate providing higher platelet activation. Asterisk (*) indicates significance with $p < 0.06$.

The coaxial electrospun scaffolds are fabricated with PVA in the core and gelatin surrounding the PVA core. Therefore, gelatin, a product of collagen hydrolysis, comes into direct contact with the external environment, in this case, the platelets. Collagen, a triple helix protein, strongly promotes the adhesion and activation of human platelets.[55] For example, human platelets and collagen fibrils in suspension showed a pseudo-first-order kinetics adhesion profile reaching 60% adhesion at 60 min of incubation.[56] Platelets can bind directly to collagen via integrin $\alpha 2\beta 1$ and glycoprotein VI as well as indirectly to collagen through von Willebrand factor. Platelet interaction and binding with collagen is dependent on the platelet receptor recognizing the protein sequence. Taking this into consideration, gelatin, a single stranded polypeptide derived from collagen, has the protein sequences needed for platelet binding; however, the single stranded structure is not recognized by these same platelet receptors as it is for collagen. Despite this, there are additional protein sequences (RGD) that are exposed in gelatin's single stranded structure that do not contribute when in the triple helix structure of collagen that may bind to platelet sites such as $\alpha 3\beta 1$, $\alpha 5\beta 1$, $\alpha V\beta 3$, and potentially $\alpha IIb\beta 3$.[57] Additionally, a study by Milleret et. al showed that fibers less than 1 μm in diameter had low platelet adhesion and coagulation.[51] Therefore, the different mechanism of platelet interaction present in the gelatin compared to collagen, as well as the nanosized fibers may account for the low PAR observed in this modified prothrombinase assay.

Platelets are able to react to the mechanical properties of the underlying substrate. Thus, platelet adhesion, spreading, and subsequent activation is greater on the stiffer substrates than the softer materials.[47] Previous studies have determined the mechanical properties of the gelatin scaffolds, PVA scaffolds,

DOI: 10.1021/acsami.5b01671
ACS Appl. Mater. Interfaces 2015, 7, 8302−8312

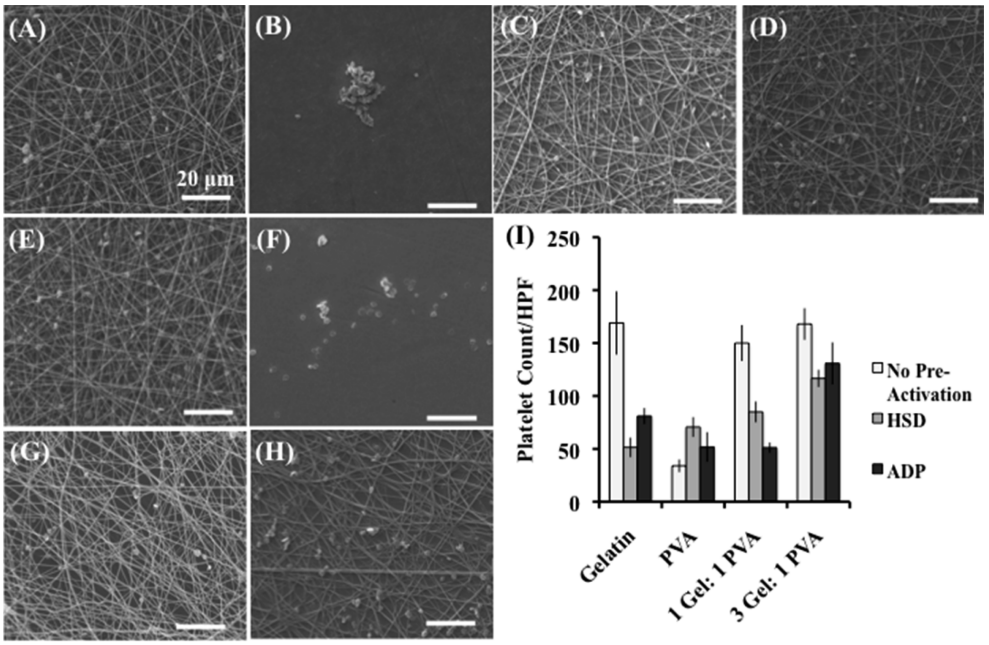

Figure 5. Deposition of platelets preactivated (A–D) mechanically (HSD) or (E–H) chemically (ADP) on defined surfaces: gelatin scaffolds (A, E), PVA scaffolds (B, F), 1 Gel:1 PVA coaxial scaffolds (C, G), and 3 Gel:1 PVA coaxial scaffolds (D, H). Platelet deposition is determined per high-powered field (HPF) (3000× magnification, approximately 8,400 μm^2). Deposition is compared with platelets that were not preactivated through mechanical (hemodynamic shearing device, HSD) or chemical (adenosine diphosphate, ADP) means (I). Scale bar equals 20 μm.

and the coaxial scaffolds (1 Gel:1 PVA and 3 Gel:1 PVA).[37,48] The coaxial scaffolds have the highest Young's modulus (3 Gel:1 PVA, 221 ± 28.4 MPa and 1 Gel:1 PVA, 168.6 ± 36.5 MPa)[37,48] and subsequently the highest PAR. In comparison to the coaxial scaffolds, gelatin has the lowest Young's modulus (21.52 ± 4.15 MPa)[37,48] and the lowest PAR. The gelatin and coaxial scaffolds (1 Gel:1 PVA coaxial and 3 Gel:1 PVA coaxial) all have gelatin external that comes into direct contact with the platelets. Therefore, when comparing these three scaffolds (i.e., gelatin, 1 Gel:1 PVA coaxial and 3 Gel:1 PVA coaxial), the mechanical stiffness of the fibers predominates in platelet activation with the stiffer substrate having the highest activation rather than the biochemical signals of gelatin.

Gelatin has the lowest Young's modulus (21.52 ± 4.15 MPa) and a similar PAR to PVA (p = 0.30). PVA has a Young's modulus of 100.5 ± 23.5 MPa; however, the PAR was low compared to the coaxial scaffolds and TCP. Although PVA has a high surface roughness and moderate stiffness compared to the gelatin and coaxial scaffolds, the PAR was low. In previous studies, we have shown that NIH 3T3 fibroblasts seeded on the PVA scaffolds had a round morphology with minimal attachment sites compared to the gelatin or coaxial scaffolds (1 Gel:1 PVA coaxial and 3 Gel:1 PVA coaxial scaffolds) that have gelatin in the shell of each nanofiber.[37] This study showed that PVA fibers do not promote the fibroblast growth and proliferation that was seen on the gelatin and coaxial scaffolds. We hypothesized that this was due to the lack of cellular attachment sites that the gelatin and gelatin coated fibers (1 Gel:1 PVA coaxial and 3 Gel:1 PVA coaxial) have in abundance.[37] A similar response was seen with the platelets having low deposition and activation on the PVA scaffolds in comparison to the gelatin and coaxial scaffolds. Overall, the PVA scaffolds do not promote cell growth and migration,[37] as well as minimize platelet activation compared to gelatin scaffolds or the coaxial scaffolds. The modified prothrombinase assay measuring platelet activation shows that the mechanical stiffness of the underlying substrate is a dominating factor in comparison to surface roughness and biochemical signals.

3.6. Platelet Deposition of Chemically or Mechanically Activated Platelets. Next, we determined platelet deposition on the nanofiber surface that was preactivated through different mechanisms (i.e., mechanical or chemical activation). We first evaluated deposition of platelets that were mechanically activated prior to incubating on the scaffolds (Figure 5A–D). The platelets were mechanically activated using a hemodynamic shear device (HSD) that exposes the platelets to dynamic shear stresses similar to the mechanical forces experienced in vivo.[39] Additionally, the HSD provides uniform and repeatable stress to the platelet samples.[45,58] In this study, the 3 Gel:1 PVA coaxial scaffold had the highest mechanically activated platelet deposition when compared to the gelatin scaffolds, PVA scaffolds, and 1 Gel:1 PVA coaxial scaffold (p < 0.03) (Figure 5I). This high platelet deposition correlated with the stiffness of the underlying substrate as discussed previously with the 3 Gel:1 PVA coaxial scaffold having the highest stiffness[37] and subsequent highest platelet deposition.

Then, platelets were chemically activated using adenosine diphosphate (ADP), a known platelet activator.[40,41] ADP activates platelets through a GTP-binding proteins or G proteins. This ADP–platelet interaction causes a platelet shape change and a decline in cAMP (cyclic adenosine monophosphate) formation, leading to platelet activation. Therefore, ADP is an important chemical factor at locations of vascular injury for the propagation of platelet activation.[59] In this study, the deposition of chemically activated platelets deposited per high-powered field (HPF) on each scaffold was calculated (Figure 5E–H). Similar to the mechanically activated platelets, the 3 Gel:1 PVA coaxial scaffolds had the highest chemically activated platelet deposition when compared with the gelatin scaffolds, PVA scaffolds, and 1 Gel:1 PVA coaxial scaffolds (p < 0.03) (Figure 5I). This high platelet deposition

DOI: 10.1021/acsami.5b01671
ACS Appl. Mater. Interfaces 2015, 7, 8302–8312

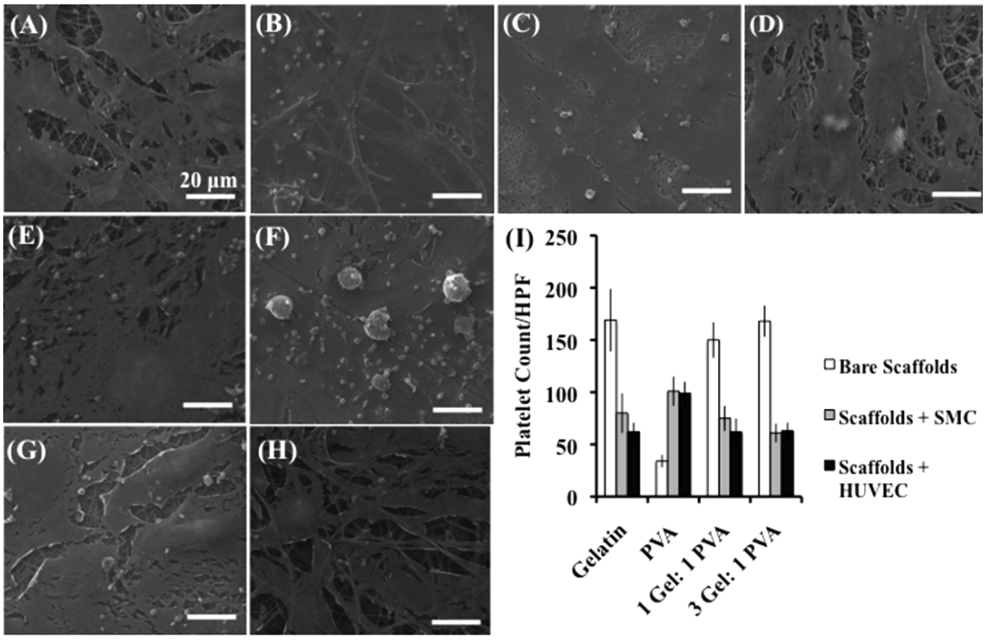

Figure 6. Platelet deposition on surfaces preseeded with smooth muscle cells (SMC) (A–D) or human umbilical vein endothelial cells (HUVEC) (E–H) on gelatin scaffolds (A, E), PVA scaffolds (B, F), 1 Gel:1 PVA coaxial scaffolds (C, G), and 3 Gel:1 PVA coaxial scaffolds (D, H). Platelet deposition is determined per high-powered field (3000×) and compared to scaffolds that were not preseeded with SMC or HUVEC (I). Scale bar equals 20 μm.

correlated with the high stiffness of the 3 Gel:1 PVA coaxial scaffolds.[37]

In this study, the preactivated platelets (both chemical and mechanical preactivation) had lower deposition on the scaffolds (gelatin, 1 Gel:1 PVA coaxial, and 3 Gel:1 PVA coaxial) than platelets that had no preactivation (Figure 5I). Platelets preactivated either mechanically or chemically undergo numerous changes, including physical shape change, exposure/activation of surface receptors, as well as secretion of chemical agonists.[60] Exposure and activation surface receptors plays a role in platelet aggregation.[60] These preactivated platelets via chemical or mechanical means had less deposition on the scaffold surface (gelatin, 1 Gel:1 PVA coaxial, and 3 Gel:1 PVA coaxial) than the platelets that were not preactivated prior to incubation. We postulated that the preactivation through chemical or mechanical means is causing platelet aggregation of the platelets in solution over the incubation period leading to less platelet deposition on the fiber surface for a given/fixed concentration of platelets.

3.7. Platelet Deposition on Electrospun Scaffolds Preseeded with SMC or HUVEC. Once the scaffold is placed in the body, vascular relevant cells (such as endothelial cells and smooth muscle cells) will begin migrating and proliferating on the fibers. Therefore, we sought to determine platelet deposition on the nanofiber surfaces when they are covered with a monolayer of smooth muscle cells or endothelial cells. First, electrospun scaffolds were preseeded with smooth muscle cells (SMC) for 72 h to ensure a confluent monolayer of cells on the scaffold surface. Once the confluent monolayer of SMC was attained, platelets were incubated for 4 h on the scaffold surfaces prior to fixation and determination of platelet deposition (Figure 6A–D). The PVA had similar platelet deposition as the gelatin scaffold (p = 0.38) and 1 Gel:1 PVA coaxial scaffold (p = 0.16), as well as significantly more platelets than the 3 Gel:1 PVA coaxial scaffold (p = 0.02). Gelatin scaffolds had similar platelet deposition to the 1 Gel:1 PVA coaxial scaffold (p = 0.22) and 3 Gel:1 PVA coaxial scaffold (p = 0.39).

Overall, there was less platelet deposition on the gelatin scaffolds (80 ± 19 platelets) and the coaxial scaffolds (1 Gel:1 PVA coaxial, 75 ± 12 platelets; 3 Gel:1 PVA coaxial, 61 ± 9 platelets) preseeded with the SMC than on the scaffolds alone (without any cell preseeding). This was not true for the PVA scaffolds, which had higher platelet deposition with the preseeding of SMC than on the scaffold fibers alone (101 ± 14 platelets with preseeding vs 34 ± 6 platelets on fibers alone). The PVA nanofibers preseeded with the smooth muscle cells, which possessed a round morphology with only a few attachment sites to the underlying nanofibers, had the highest platelet deposition. In contrast, the smooth muscle cells on the gelatin and coaxial scaffolds possessed a flattened morphology with numerous attachment sites, decreasing the platelet deposition in comparison to scaffolds with no cell preseeding.

Electrospun scaffolds were preseeded with HUVEC for 72 h to allow the cells to proliferate and form a confluent monolayer. After the 72 h of incubation, the cells were incubated with platelets for 4 h and subsequently prepared for SEM imaging and counting (Figure 6E–H). A similar trend was observed for the HUVEC preseeding as was seen with the SMC preseeding (Figure 6I). The PVA had the highest platelet deposition (99 ± 11 platelets), whereas the gelatin (62 ± 9 platelets), 1 Gel:1 PVA coaxial (62 ± 13 platelets), and 3 Gel:1 PVA coaxial (63 ± 8 platelets) scaffolds had similar and lower depositions than platelet deposition on the scaffold fibers alone.

Studies have shown the antithrombogenic properties of the native endothelium such as the release of nitric oxide (NO) and prostacyclin to decrease platelet activation and adhesion.[61,62] Therefore, the scaffolds (i.e., gelatin, 1 Gel:1 PVA coaxial, and 3 Gel:1 PVA coaxial) that had a confluent monolayer of endothelial cells similar to the native vasculature displayed a decline in platelet deposition compared to the scaffolds with no endothelial preseeding. Interestingly, scaffolds that were

DOI: 10.1021/acsami.5b01671
ACS Appl. Mater. Interfaces 2015, 7, 8302–8312

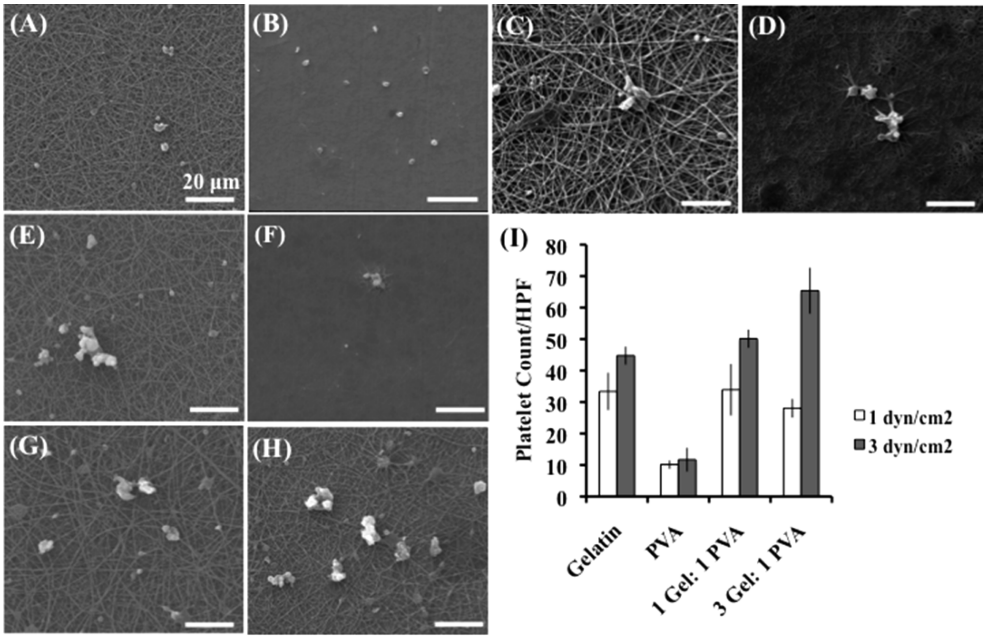

Figure 7. Platelet deposition on electrospun scaffolds under shear, 1 dyn/cm^2 (A–D) and 3 dyn/cm^2 (E–H). Platelet deposition was calculated on the following scaffolds per high powered field (3000×): gelatin scaffolds (A, E), PVA scaffolds (B,F), 1 Gel:1 PVA coaxial scaffolds (C, G), 3 Gel:1 PVA coaxial scaffolds (D, H). Platelet deposition on gelatin, PVA, 1 Gel:1 PVA coaxial, or 3 Gel: 1 PVA coaxial scaffolds under shear (1 or 3 dyn/cm^2) is presented in this bar graph per high-powered field (3000×) (I). Scale bar 20 μm.

preseeded with smooth muscle cells also showed a decline in platelet deposition. After vascular injury, various mitogenic and chemotactic factors are released from the wound area, as well as from aggregated platelets that are on the damaged intimal surface. These factors will initiate the neointimal response.[63] We hypothesized that in the absence of vascular injury, cell preseeding would reduce platelet deposition for gelatin and gelatin-coated fibers, as was observed for both endothelial cells and smooth muscle cells respectively in this experiment.

In contrast, platelet deposition increased on the PVA scaffolds that were preseeded with endothelial cells or smooth muscle cells. Endothelial cells, smooth muscle cells, and/or fibroblasts produce components involved in the hemostatic response in vivo.[64] Previous studies have shown low cell attachment of 3T3 fibroblasts on the PVA scaffolds.[37] With low cell attachment at the time of platelet deposition, we hypothesized that the hemostatic balance was no longer maintained, thereby making these surfaces more thrombogenic than the PVA fibers alone. Overall, the formation of a confluent monolayer of SMC or HUVEC decreased platelet deposition than on the scaffolds alone, suggesting that the nanofibrous scaffold has proadhesive and antithrombogenic properties for cells and platelets, respectively.

3.8. Platelet Deposition on Electrospun Scaffolds under Flow. Areas of low wall shear stress in the coronary arteries tend to have an increase in plaque accumulation, as well as an increase in necrotic core. The low wall shear stress results in a decrease in alignment of the endothelial cells to the flow axis, as well as an increase in low-density lipoproteins (LDL), smooth muscle cell proliferation, and macrophage migration.[65] Therefore, understanding platelet deposition on the electrospun surfaces under flow conditions is vital for vascular applications. For this experiment, we electrospun the scaffolds (gelatin, PVA, 1 Gel:1 PVA coaxial, and 3 Gel:1 PVA coaxial) onto stainless steel chips, cross-linked the scaffolds with glutaraldehyde vapor, and placed the chips into a parallel plate flow chamber.[42] A pulsatile pump is used to circulate platelet-rich plasma (PRP) through the flow loop at either 1 dyn/cm^2 (Figure 7A–D) or 3 dyn/cm^2 (Figure 7E–H). After the PRP circulates through the flow loop, the scaffolds and stainless steel chips are removed, fixed, and prepared for SEM imaging (Figure 7). Platelet counts per high-powered field (3000×) are calculated as previously described (Figure 7I).

In a study conducted by Badimon et al., a de-endothelialized vessel wall showed an increase in platelet deposition with an increase in exposure time and shear.[66] Taking only flow rate into consideration, the increase in shear will activate platelets mechanically, leading to an increase in platelet deposition.[67] Herein, we also observed the latter published results, where platelet deposition increased when the shear was increased from 1 to 3 dyn/cm^2 for the 3 Gel:1 PVA coaxial scaffolds ($p < 0.001$) with less significance seen in the 1 Gel:1 PVA coaxial scaffolds ($p < 0.07$) and gelatin scaffolds ($p < 0.09$). We postulate that the mechanical shear stress not only induced platelet activation but also mobilized them toward the scaffolds, such that an increase in platelet deposition was observed with an increase in shear stress.

Overall, platelet deposition under shear conditions was still much less than static conditions. For instance, PVA had the least platelet deposition of all the scaffolds for the static conditions (Figure 6I, bare scaffold), as well as the shear conditions (Figure 7I, 1 or 3 dyn/cm^2). This low platelet deposition for the static and shear conditions was attributed to the hydrophilic nature of PVA and poor cellular attachment and proliferative nature of the PVA scaffolds,[37] Ikada et al. showed that there was less platelet deposition and fibrin formation using PRP than on nongrafted and acrylic acid-grafted polyethylene.[68] Overall, the platelet deposition was significantly decreased under shear than in static conditions, suggesting that the scaffolds perform better under dynamic flow than in a static environment.

DOI: 10.1021/acsami.5b01671
ACS Appl. Mater. Interfaces 2015, 7, 8302–8312

4. CONCLUSION

In this study, we fabricated coaxial nanofibers composed of gelatin in the shell and poly(vinyl alcohol) (PVA) in the core of each fiber and evaluated its hemocompatibility by determining platelet deposition and activation under varying conditions. We hypothesized that the coaxial nanofibers with gelatin in the shell and PVA in the core would be an optimal construct for vascular applications, displaying minimal platelet deposition and activation. First, PVA nanofibers had the highest surface roughness (Ra) in comparison to gelatin and the coaxial scaffolds (1 Gel:1 PVA coaxial fibers and 3 Gel:1 PVA coaxial fibers). Despite the highest surface roughness, the PVA scaffolds had the lowest platelet deposition under static conditions out of all of the scaffolds (gelatin, PVA, 1 Gel:1 PVA coaxial, and 3 Gel:1 PVA coaxial). Therefore, the biochemical signals of gelatin dominated surface roughness for platelet deposition on these electrospun fibers. Next, the modified-prothrombinase assay was used to determine the rate of thrombin formation of platelets on the scaffolds. Overall, the coaxial scaffolds had the highest platelet activation rate of the electrospun fibers, which was followed by gelatin and PVA scaffolds. The increase in platelet activation rate correlated with the increase in stiffness of the underlying fibers. Therefore, platelet activation of fibers with the same surface chemistry (i.e., gelatin external) is dominated by mechanical stiffness of the underlying substrate. Our experiments show that the following factors influence platelet deposition and activation on the fibers in order significance: mechanical stiffness followed by biochemical signals, and lastly surface roughness. Additionally, when the scaffolds were preseeded with either SMC or HUVEC, the platelet deposition decreased significantly on the gelatin and coaxial scaffolds. In contrast, preseeding with the SMC or HUVEC increased platelet deposition on the PVA scaffolds. Overall, the 1 Gel:1 PVA coaxial scaffolds, promoting cellular viability and growth, as well as minimal platelet deposition and activation, possess appealing hemocompatibility for use in vascular applications.

AUTHOR INFORMATION

Corresponding Authors

*X. Wu. Tel.: 1-520-626-5854. Fax: 1-00-520-621-8191.
*M. J. Slepian. Tel.: +1 520-626-8543.

Author Contributions

The paper was written through contributions of all authors. All authors have given approval to the final version of the paper.

Funding

Funding was provided by NIBIB EB009160, NIH grant 5U01EB012487, and The University of Arizona Bio5 Seed Grant U01 EB012487.

Notes

The authors declare no competing financial interest.

ACKNOWLEDGMENTS

The authors thank Samir Mohandes and Jonathan Yamaguchi for assistance in scanning electron microscopy preparation and imaging, as well as Walter Merkle for assistance in experiment preparation and data collection. Additionally, the authors thank David You for fabrication of the parallel plate flow chamber.

REFERENCES

(1) WHO Cardiovascular diseases (CVDs). http://www.who.int/mediacentre/factsheets/fs317/en/index.html (accessed July 7, 2013).

(2) Go, A. S.; Mozaffarian, D.; Roger, V. R. L.; Benjamin, E. J.; Berry, J. D.; Borden, W. B.; Bravata, D. M.; Dai, S.; Ford, E. S.; Fox, C. S.; Franco, S.; Fullerton, H. J.; Gillespie, C.; Hailpern, S. M.; Heit, J. A.; Howard, V. J.; Huffman, M. D.; Kissela, B. M.; Kittner, S. J.; Lackland, D. T.; Lichtman, J. H.; Lisabeth, L. D.; Magid, D.; Marcus, G. M.; Marelli, A.; Matchar, D. B.; McGuire, D. K.; Mohler, E. R.; Moy, C. S.; Mussolino, M. E.; Nichol, G.; Paynter, N. P.; Schreiner, P. J.; Sorlie, P. D.; Stein, J.; Turan, T. N.; Virani, S. S.; Wong, N. D.; Woo, D.; Turner, M. B. Heart Disease and Stroke Statistics—2013 Update: A Report From the American Heart Association. *Circulation* **2013**, *127*, 6−245.

(3) Zong, X. H.; Bien, H.; Chung, C. Y.; Yin, L. H.; Fang, D. F.; Hsiao, B. S.; Chu, B.; Entcheva, E. Electrospun Fine-Textured Scaffolds for Heart Tissue Constructs. *Biomaterials* **2005**, *26*, 5330−5338.

(4) Tan, A.; Farhatnia, Y.; de Mel, A.; Rajadaas, J.; Alavijeh, M. S. Inception to Actualization: Next Generation Coronary Stent Coatings Incorporating Nanotechnology. *J. Biotechnol.* **2013**, *164*, 151−170.

(5) Caramori, P. R. A.; Lima, V. C.; Seidelin, P. H.; Newton, G. E.; Parker, J. D.; Adelman, A. G. Long-Term Endothelial Dysfunction after Coronary Artery Stenting. *J. Am. Coll. Cardiol.* **1999**, *34*, 1675−1679.

(6) Study Tallies Risk of Noncardiac Surgery After Heart Stent Placement. http://health.usnews.com/health-news/news/articles/2013/10/07/study-tallies-risk-of-noncardiac-surgery-after-heart-stent-placement (accessed March 10, 2014).

(7) Nakazawa, G.; Vorpahl, M.; Finn, A. V.; Narula, J.; Virmani, R. One Step Forward and Two Steps Back with Drug-Eluting-Stents. *JACC* **2009**, *2*, 625−628.

(8) vom Dahl, J.; Haager, P. K.; Grube, E.; Gross, M.; Beythien, C.; Kromer, E. P.; Cattelaens, N.; Hamm, C. W.; Hoffman, R.; Reineke, T.; Klues, H. G. Effects of Gold Coating of Coronary Stents on Neointimal Proliferation Following Stent Implantation. *Am. J. Cardiol.* **2002**, *89*, 801−805.

(9) Mani, G.; Feldman, M. D.; Patel, D.; Agrawal, C. M. Coronary Stents: A Materials Perspective. *Biomaterials* **2007**, *28*, 1689−1710.

(10) Babapulle, M. N.; Eisenberg, M. J. Coated Stents for the Prevention of Restenosis: Part II. *Circulation* **2002**, *106*, 2859−2866.

(11) O'Brien, B.; Carroll, W. The Evolution of Cardiovascular Stent Materials and Surfaces in Response to Clinical Drivers: A Review. *Acta Biomater.* **2009**, *5*, 945−958.

(12) Unverdorben, M.; Sattler, K.; Degenhardt, R.; Fries, R.; Abt, B.; Wagner, E.; Koehler, H.; Daemgen, G.; Scholz, M.; Ibrahim, H.; Tews, K. H.; Hennen, B.; Berthold, H. K.; Vallbracht, C. Comparison of Silicon Carbide Coated Stent versus a Noncoated Stent in Humans: The Tenax-versus Nir-Stent Study. *J. Interventional Cardiol.* **2003**, *16*, 325−333.

(13) Hoffman, R.; Langenberg, R.; Radke, P.; Franke, A.; Blindt, R.; Ortlepp, J.; Popma, J. J.; Weber, C.; Hanrath, P. Evaluation of a High-Dose Dexamethasone-Eluting Stent. *Am. J. Cardiol.* **2004**, *94*, 193−195.

(14) Lee, W. L.; Chae, J.-K.; Lim, H.-Y.; Hong, M.; Kim, J.-J.; Park, S.-W.; Park, S.-J. Prospective Randomized Trial of Corticosteroids for the Prevention of Restenosis after Intracoronary Stent Implantation. *Am. Heart J.* **1998**, *138*, 60−63.

(15) Farhatnia, Y.; Tan, A.; Motiwala, A.; Cousins, B. G.; Seifalian, A. M. Evolution of Covered Stents in the Contemporary Era: Clinical Application, Materials and Manufacturing Strategies Using Nanotechnology. *Biotechnol. Adv.* **2013**, *31*, 524−542.

(16) Takano, M.; Yamamoto, M.; Inami, S.; Xie, Y.; Murakami, D.; Okamatsu, K.; Ohba, T.; Seino, Y.; Mizuno, K. Delayed Endothelialization after Polytetrafluoroethylene-Covered Stent Implantation for Coronary Aneurysm. *Circ. J.* **2009**, *73*, 190−193.

(17) Briguori, C.; Nishida, T.; Anzuini, A.; DiMario, C.; Grube, E.; Colombo, A. Emergency Polytetrafluoroethylene-Covered Stent Implantation to Treat Coronary Ruptures. *Circulation* **2000**, *102*, 3028−3031.

(18) Sarkar, S.; Salacinski, H.; Hamilton, G.; Seifalian, A. The Mechanical Properties of Infrainguinal Vascular Bypass Grafts: Their

DOI: 10.1021/acsami.5b01671
ACS Appl. Mater. Interfaces 2015, 7, 8302−8312

Role in Influencing Patency. *Eur. J. Vasc. Endovasc. Surg.* **2006**, *31*, 627−636.
(19) Marty, B.; Leu, A.; Mucciolo, A.; von Segesser, L. Biologic Fixation of Polyester- versus Polyurethane-Covered Stents in a Porcine Model J. Vasc. *J. Vasc. Interventional Radiol.* **2002**, *13*, 601−607.
(20) Bhardwaj, N.; Kundu, S. C. Electrospinning: A Fascinating Fiber Fabrication Technique. *Biotechnol. Adv.* **2010**, *28*, 325−347.
(21) Greiner, A.; Wendorff, J. H. Electrospinning: A Fascinating Method for the Preparation of Ultrathin Fibres. *Angew. Chem., Int. Ed.* **2007**, *46*, 5670−5703.
(22) Naito, Y.; Shinoka, T.; Duncan, D.; Hibino, N.; Solomon, D.; Cleary, M.; Rathore, A.; Fein, C.; Church, S.; Breuer, C. Vascular Tissue Engineering: Towards the Next Generation Vascular Grafts. *Adv. Drug Delivery Rev.* **2011**, *63*, 312−323.
(23) Tillman, B. W.; Yazdani, S. K.; Lee, S. J.; Geary, R. L.; Atala, A.; Yoo, J. J. The in Vivo Stability of Electrospun Polycaprolactone-Collagen Scaffolds in Vascular Reconstruction. *Biomaterials* **2009**, *30*, 583−588.
(24) Feng Wang; Guo, E.; Song, E.; Zhao, P.; Liu, J. Structure and Properties of Bone-like-Nanohydroxyapatite/Gelatin/Polyvinyl Alcohol Composites. *Adv. Biosci. Biotechnol.* **2010**, *1*, 185−189.
(25) Linh, N. T.; Lee, B. T. Electrospinning of Polyvinyl Alcohol/Gelatin Nanofiber Composites and Cross-Linking for Bone Tissue Engineering Application. *J. Biomater. Appl.* **2012**, *27*, 255−66.
(26) Linh, N. T. B.; Min, Y. K.; Song, H.-Y.; Lee, B.-T. Fabrication of Polyvinyl Alcohol/Gelatin Nanofiber Composites and Evaluation of Their Material Properties. *J. Biomed. Mater. Res., Part B* **2010**, *95B*, 184−191.
(27) Nien, Y. H.; Chen, Z. B.; Liang, J. I.; Yeh, M. L.; Hsu, H. C.; Su, F. C. Fabrication and Cell Affinity of Poly(vinyl alcohol) Nanofibers via Electrospinning. *J. Med. Biol. Eng.* **2009**, *29*, 98−101.
(28) Sisson, K.; Zhang, C.; Farach-Carson, M. C.; Chase, D. B.; Rabolt, J. F. Evaluation of Cross-Linking Methods for Electrospun Gelatin on Cell Growth and Viability. *Biomacromolecules* **2009**, *10*, 1675−80.
(29) Zha, Z.; Teng, W.; Markle, V.; Dai, Z.; Wu, X. Fabrication of Gelatin Nanofibrous Scaffolds Using Ethanol/Phosphate Buffer Saline As a Benign Solvent. *Biopolymers* **2012**, *97*, 1026−1036.
(30) Pham, Q. P.; Sharma, U.; Mikos, A. G. Electrospinning of Polymeric Nanofibers for Tissue Engineering Applications: A Review. *Tissue Eng.* **2006**, *12*, 1197−1211.
(31) Venugopal, J.; Ramakrishna, S. Applications of Polymer Nanofibers in Biomedicine and Biotechnology. *Appl. Biochem. Biotechnol.* **2005**, *125*, 147−58.
(32) Zhang, H.; Zhao, C.; Zhao, Y.; Tang, G.; Yuan, X. Electrospinning of Ultrafine Core/Shell Fibers for Biomedical Applications. *Sci. Chem. China* **2010**, *53*, 1246−1254.
(33) Su, Y.; Su, Q.; Liu, W.; Jin, G.; Mo, X.; Ramakrishna, S. Dual-Drug Encapsulation and Release from Core-Shell Nanofibers. *J. Biomater. Sci., Polym. Ed.* **2011**, *23*, 861−871.
(34) Schmedlen, R.; KS, M.; JL, W. Photocrosslinkable Polyvinyl Alcohol Hydrogels that Can be Modified with Cell Adhesion Peptides for Use in Tissue Engineering. *Biomaterials* **2002**, *23*, 4325−4332.
(35) Zhang, Y. Z.; Venugopal, J.; Huang, Z.-M.; Lim, C. T.; Ramakrishna, S. Characterization of the Surface Biocompatibility of the Electrospun PCL-Collagen Nanofibers Using Fibroblasts. *Biomacromolecules* **2005**, *6*, 2583−2589.
(36) Zhao, P.; Jiang, H.; Pan, H.; Zhu, K.; Chen, W. Biodegradable Fibrous Scaffolds Composed of Gelatin Coated Poly(e-caprolactone) prepared by Coaxial Electrospinning. *J. Biomed. Mater. Res., Part A* **2007**, 372−382.
(37) Merkle, V. M.; Zeng, L.; Slepian, M. J.; Wu, X. Core-Shell Nanofibers: Integrating the Bioactivity of Gelatin and the Mechanical Property of Polyvinyl Alcohol. *Biopolymers* **2014**, *101*, 336−346.
(38) Mehta, J. L. *Thrombosis and Platelets in Myocardial Ischemia*; F.A. Davis Company: Philadelphia, 1987.
(39) Nobili, M.; Sheriff, J.; Morbiducci, U.; Redaelli, A.; Bluestein, D. Platelet Activation Due to Hemodynamic Shear Stresses: Damage Accumulation Model and Comparision to in Vitro Measurements. *ASAIO J.* **2008**, *54*, 64−72.
(40) Angiolillo, D. J.; Ueno, M.; Goto, S. Basic Principles of Platelet Biology and Clinical Implications. *Circ. J.* **2010**, *74*, 597−607.
(41) Jennings, L. K. Mechanisms of Platelet Activation: Need for New Strategies to Protect against Platelet-Mediated Atherothrombosis. *Thromb. Haemostasis* **2009**, *102*, 248−257.
(42) Bacabac, R. G.; Smit, T. H.; Cowin, S. C.; Van Loon, J. J. W. A.; Nieuwstadt, F. T. M.; Heethaar, R.; Klein-Nulend, J. Dynamic Shear Stress in Parallel-Plate Flow Chambers. *J. Biomech.* **2005**, *38*, 159−167.
(43) Park, J.; Lakes, R. S. *Biomaterials: An Introduction*, 3rd ed.; Springer: New York, 2007.
(44) Jesty, J.; Bluestein, D. Acetylated Prothrombin as a Substrate in the Measurement of the Procoagulant Activity of Platelets: Elimination of the Feedback Activation of Platelets by Thrombin. *Anal. Biochem.* **1999**, *272*, 64−70.
(45) Sheriff, J.; Bluestein, D.; Girdhar, G.; Jesty, J. High-Shear Stress Sensitizes Platelets to Subsequent Low-Shear Conditions. *Ann. Biomed. Eng.* **2010**, *38*, 1442−1450.
(46) Nobili, M.; Sheriff, J.; Morbiducci, U.; Redaelli, A.; Bluestein, D. Platelet Activation due to Hemodynamic Shear Stresses: Damage Accumulation Model and Comparison to in Vitro Measurements. *ASAIO J.* **2008**, *54*, 64−72.
(47) Qiu, Y.; Brown, A. C.; Jung, W. J.; Sakurai, Y.; Mannino, R.; Myers, D. R.; Tran, R.; Bao, G.; Barker, T. H.; Lam, W. Platelet Mechanosensing: Adhesion and Spreading on Immobilized Fibrinogen Depends on Substrate Stiffness, *54th ASH Annual Meeting and Exposition*, Atlanta, GA, December 8−11, 2012.
(48) Merkle, V.; Zeng, L.; Teng, W.; Slepian, M.; Wu, X. Gelatin Shells Strengthen Polyvinyl Alcohol Core-Shell Nanofibers . *Polymers* **2013**, *54*, 6003−6007.
(49) Thomasson, S. A.; Thomasson, J. R. A Comparison of CPD (Critical Point Drying) and HMDS (Hexamethyldisilazane) in the Preparation of *Corallorhiza* spp. Rhizomes and Associated Mycorrhizae for SEM (Scanning Electron Microscopy). *Trans. Kans. Acad. Sci.* **2011**, *114*, 129−134.
(50) Rubenstein, D. A.; Venkitachalam, S. M.; Zamfir, D.; Wang, F.; Lu, H.; Frame, M. D.; Yin, W. In Vitro Biocompatibility of Sheath−Core Cellulose-Acetate-based Electrospun Scaffolds towards Endothelial Cells and Platelets. *J. Biomater. Sci., Polym. Ed.* **2010**, *21*, 1713−1736.
(51) Milleret, V.; Hefti, T.; Hall, H.; Vogel, V.; Eberli, D. Influence of the Fiber Diameter and Surface Roughness of Eletcrospun Vascular Grafts on Blood Activation. *Acta Biomater.* **2012**, *8*, 4349−4356.
(52) Fatisson, J.; Mansouri, S.; Merhi, Y.; Tabrizian, M. Determination of Surface-Induced Platelet Activation by Applying Time-Dependency Dissipation Factor versus Frequency Using Quartz Crystal Microbalance with Dissipation. *J. R. Soc., Interface* **2011**, *8*, 1−10.
(53) Naghadeh, H. T.; Badlou, B. A.; Ferizhandy, A. S.; Mohammadreza, T. S.; Shahram, V. Six Hours of Resting Platelet Concentrates Stored at 22−24 °C for 48 h in Permeable Bags Preserved pH, Swirling and Lactate Dehydrogenase Better and Caused Less Platelet Activation. *Blood Transfus.* **2013**, *11*, 400−404.
(54) Gupta, A.; Chandra, T.; Kumar, A. In Vitro Function of Random Donor Platelets Stored for 7 Days in Composol Platelet Additive Solution Asian. *J. Transfus. Sci.* **2011**, *5*, 160−163.
(55) Cosemans, J. M. E. M.; Kuijpers, M. J. E.; Lecut, C.; Loubele, S. T. B. G.; Heeneman, S.; Jandrot-Perrus, M.; Heemskerk, J. W. M. Contribution of Platelet Glycoprotein VI to the Thrombogenic Effect of Collagens in Fibrous Atherosclerotic Lesions. *Atherosclerosis* **2005**, *181*, 19−27.
(56) Dolowy, K.; Cunningham, L. W. Adhesion of Human Platelets to Collagen: Evidence for Two States of Platelet Activation. *Collagen Relat. Res.* **1984**, *4*, 111−118.
(57) Farndale, R. W. Collagen-Induced Platelet Activation. *Blood Cells, Mol., Dis.* **2006**, *36*, 162−165.
(58) Nobili, M.; Sheriff, J.; Morbiducci, U.; Redaelli, A.; Bluestein, D. Platelet Activation Due to Hemodynamic Shear Stresses: Damage

DOI: 10.1021/acsami.5b01671
ACS Appl. Mater. Interfaces 2015, 7, 8302−8312

Accumulation Model and Comparison to in Vitro Measurements. *ASAIO J.* **2008**, *54*, 64−72.
(59) Woulfe, D.; Yang, J.; Brass, L. ADP and Platelets - The End of the Beginning. *J. Clin. Invest.* **2001**, 107.
(60) Gregg, K. L. A Mathmatical Model of Blood Coagulation and Platelet Deposition Under Flow. Ph.D. Dissertation, The University of Utah, Salt Lake City, UT, 2010.
(61) Landmesser, U.; Burkhard, H.; Drexler, H. Vascular Effects of Statins . *Circulation* **2004**, *109*, II-27−II-33.
(62) Loscalzo, J. Nitric Oxide Insufficiency, Platelet Activation, and Arterial Thrombosis. *Circ. Res.* **2001**, *88*, 756−762.
(63) Louis, S. F.; Zahradka, P. Vascular Smooth Muscle Cell Motility: From Migration to Invasion. *Exp. Clin. Cardiol.* **2010**, *15*, e75−e85.
(64) Zwaginga, J. J.; de Boer, H. C.; IJsseldijk, M. J.; Kerkhof, A.; Muller-Berghaus, G.; Gruhlichhenn, J.; Sixma, J. J.; Groot, P. G. d. Thrombogenicity of Vascular Cells. Comparison between Endothelial Cells Isolated from Different Sources and Smooth Muscle Cells and Fibroblasts. *Arteriosclerosis* **1990**, *10*, 437−448.
(65) Samady, H.; Eshtehardi, P.; McDaniel, M. C.; Suo, J.; Dhawan, S. S.; Maynard, C.; Timmins, L. H.; Quyyumi, A. A.; Giddens, D. P. Coronary Artery Wall Shear Stress Is Associated With Progression and Transformation of Atherosclerotic Plaque and Arterial Remodeling in Patients With Coronary Artery. *Disease Circulation* **2011**, *124*, 779−788.
(66) Badimon, L.; Badimon, J.; Galvez, A.; Chesebro, J.; Fuster, V. Influence of Arterial Damage and Wall Shear Rate on Platelet Deposition. Ex Vivo Study in a Swine Model. *Arteriosclerosis* **1986**, *6*, 312−320.
(67) Colman, R. W.; Marder, V. J.; Clowes, A. W.; George, J. N.; Goldhaber, S. Z. *Hemostasis and Thrombosis: Basic Principles and Clinical Practice*, 5 ed.; Lippincott Williams & Wilkins: Philadelphia, 2006.
(68) Ikada, Y.; Iwata, H.; Horii, F.; Matsunaga, T.; Taniguchi, M.; Taki, W.; Yamagata, S.; Yonekawa, Y.; Handa, H. Blood Compatibility of Hydrophilic Polymers. *J. Biomed. Mater. Res.* **1981**, *15*, 697−718.

DOI: 10.1021/acsami.5b01671
ACS Appl. Mater. Interfaces 2015, 7, 8302−8312